

## Experimental study of heat and mass transfer in a fixed-bed dryer

Hani Nassari<sup>1</sup>, Alireza Azimi<sup>2,\*</sup><sup>1,2</sup>Department of Chemical Engineering, Mahshahr Branch, Islamic Azad University, Mahshahr, Iran;

\*corresponding author e-mail address: Alireza\_azimi550@yahoo.com

## ABSTRACT

In this work, a fixed-bed dryer was manufactured and used to dry silica gel particles. The heat needed to drying of silica gel particles was provided by hot air. The relative humidity and air temperature of the dryer inlet and outlet were continuously recorded by Graph View Vista 3.0.5 and transferred to a computer. The air flow rate was 15 to 43 cubic meters per hour, and the temperature ranged between 75 and 100°C. The kinetic parameters of drying of silica gel were investigated in the fixed-bed dryer. The experimental results showed that increase in the flow rate increased the mass and heat transfer coefficients, while the diffusivity of water in the air remained almost constant. The increased temperature leads to increase in the heat transfer coefficient and the mass transfer coefficient, as well as the diffusivity. The obtained mass transfer coefficient ranged from 0.35 to 0.39 m/s. Heat transfer coefficient ranged from 19 to 28 W/m<sup>2</sup>.K. Experimental results were statistically analyzed by the Design Expert software, and an empirical relationship was proposed for predicting the heat transfer coefficient (h) and the mass transfer coefficient (K<sub>c</sub>).

**Keywords:** heat and mass transfer; fixed-bed dryer; silica gel; kinetic parameters.

## 1. INTRODUCTION

Drying is an important industrial process. It is widely used in the chemical industry, especially in the food industry. Another important application of drying is the removal of water from adsorbents such as silica gel and zeolites. Thus, reusing these adsorbents is more cost effective than using new adsorbent. There are several methods for drying important industrial adsorbents [1-5]. Hashemi et al. examined the kinetics of drying of parsley using fixed-bed dryer and the artificial neural network method. Parsley leaves were dried at temperatures of 85, 64 and 54°C, thicknesses of 0.13-0.15 mm, and time interval of 0 to 180 minutes in a fixed laboratory bed under sunlight. A comparison was made between the drying rate of parsley leaves by the machine and under sunlight. The parsley drying process was then modeled using neural networks [6]. Rahmanian et al. (2017) experimentally and theoretically examined the drying of corn using hot air in fixed-bed and vibrating-bed dryers. The effects of inlet air temperature and infrared radiation (1000, 2000, and 3000 w/m<sup>2</sup>) in both fixed and vibrating beds on changes in moisture content of corn during the drying process were investigated. Corn kernels were dried from the initial moisture content of 24.5% to the final moisture content of 14%. Among the models derived from empirical data, the plate model was found to be the best model to describe corn drying behavior [7]. Pusat et al. (2015)

experimentally studied the kinetics of coarse coal particles drying in a fixed-bed using the multiple regression analysis. Drying experiments were carried out at air temperatures of 70, 100 and 130°C, air velocities of 0.4, 1.7, and 1.1 m/s, and sample size of 20, 35, and 50 mm. The results of the models were evaluated using statistical analyses. Results showed that the model by Wang and Singh was the best for describing the kinetics of drying konya-IIgin coal under different drying conditions (temperature, velocity, and sample height and size) in a fixed-bed dryer [8]. Tohidi et al. (2017) examined drying of rice in fixed beds. The freshly harvested rice was studied in a fixed-bed dryer under different conditions. Drying experiments on freshly harvested rice were conducted at different air flows, as well as parameters such as temperature, velocity, and relative humidity. Results show that any increase in the temperature and velocity of the drying air can reduce the drying time, while higher levels of relative humidity increased the drying time. The total energy consumption ranged from 1.85 kWh to 0.37 kWh, while the minimum and maximum values corresponded to the experiments at T=80 C°, V=0.5 m/s, RH=40%, and T=40 C°, V=1.1 m/s, RH=70%, respectively. Results showed that drying of rice at higher temperature, lower air velocity, and lower air relative humidity leads to higher energy efficiency [9].

## 2. THEORY

## 2.1. Determination of heat transfer coefficient (h).

(For the parallel flow of air over the surface of a substance, if the air temperature ranges between 45 and 150 and the air velocity ranges between 0.61 and 7.6  $\frac{m}{s}$ , heat transfer coefficient is calculated using the following empirical relationship:

$$h = 0.0204 G^{0.8} \quad (1)$$

The heat transfer coefficient unit in SI system is  $\frac{W}{m^2 \cdot K}$ .

For the vertical flow of air over the surface of the particles, the heat transfer coefficient is calculated using the following empirical relationship:

$$h = 1.17 G^{0.37} \quad (2)$$

In equations (1) and (2), G represents the mass flux with

the unit  $\frac{kg}{m^2.hr}$ .

## 2.2. Calculation of bulk properties.

### Porosity

To calculate the bulk porosity gravimetric method is used. The Porosimeter "PASCAL 140" used to measure the porosity of the particles. In addition, the average porosity for each particle diameter was calculated [10]:

$$\varepsilon = (\text{volume of pores} / \text{total volume}) \quad (3)$$

If we denote the total volume by  $V_t$  and the volume of the pores by  $V_p$  and the volume of particles by  $V_s$ , according to the definition of porosity [10]:

$$\varepsilon = \frac{V_p}{V_t} = \frac{V_t - V_s}{V_t}$$

### 2.3. Calculation of effective diffusion coefficient ( $D_{eff}$ ).

The following relation is applied to calculate the effective diffusion coefficient:

$$D_{eff} = \frac{D_{AB}}{\tau} \quad (5)$$

### 2.4. Determination of mass transfer coefficient ( $K_C$ ).

The mass transfer coefficient ( $K_C$ ) must be calculated using relationships and assumptions.

For a gas flowing around a spherical particle in a fixed-bed, the followed correlation was suggested [13-17].

$$J_D = \frac{2.06}{\varepsilon} Re^n \quad Re^n = 90 - 4000 \quad (7)$$

Where,  $Re^n$  is the Reynolds number around the sphere. [15].

$$Re^n = \frac{G'.d_p}{\mu} = \frac{\rho.u.d_p}{\mu} \quad (8)$$

## 3. EXPERIMENT

### 3.1. Materials.

The blue silica gel indicator produced were purchased from Derakhshan Company. Blue silica gel is produced in two forms granular (irregular) and spherical in different sizes (Fig.1):

Physical properties of blue silica gel are summarized in Table 1.

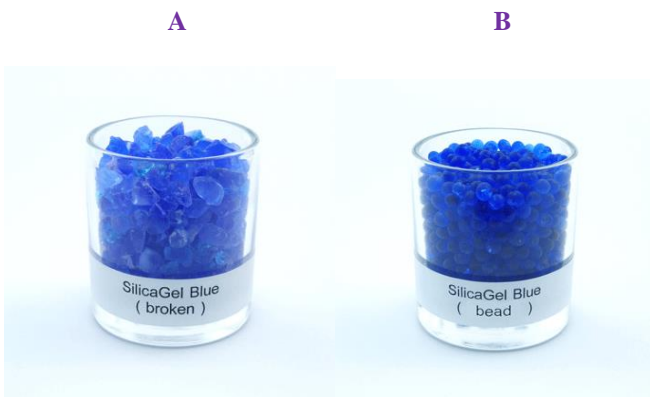


Figure 1. Blue Silica Gel: (A) Granular, (B) Spherical.

Which,  $\varepsilon$  is porosity,  $\tau$  is tortuosity of the particle, which is taken as relation (5). [11]:

The Wilke-Lee relationship is presented for the diffusion of a polar gas into a mixture of non-polar gases [12]:

$$D_{AB} = \frac{2 \times 10^{-22} \left( 1.084 - 0.249 \sqrt{\left( \frac{1}{M_A} + \frac{1}{M_B} \right)} \right) T^{\frac{3}{2}} \sqrt{\left( \frac{1}{M_A} + \frac{1}{M_B} \right)}}{P_i (r_{AB})^2 \cdot f \left( \frac{kT}{\varepsilon_{AB}} \right)} \quad (6)$$

The values for  $r_{AB} = \frac{r_A + r_B}{2}$  and  $f \left( \frac{kT}{\varepsilon_{AB}} \right)$  were determined using the tables available in the literature [12].

Schmidt number is calculated as follows:

$$Sc = \frac{\mu}{\rho.D_{AB}} \quad (9)$$

The relationship between Sherwood number and the mass transfer coefficients is as follows [18]:

$$Sh = \frac{F.D}{C.D_{AB}} = \frac{K_C \cdot \bar{P}_{BM} \cdot d_p}{D_{AB}} \cdot \frac{RT}{P_i} \quad (10)$$

$$J_D = St_D \cdot Sc^{2/3} = \frac{Sh}{Re \cdot Sc} Sc^{2/3} \quad (11)$$

Table 1. Physical Properties of Blue Silica Gel.

Bulk Density	700-800 g/L
Specific Surface Area,	700-750 m <sup>2</sup> /g
Dry Weight Loss	%2>
Particle Diameter	3-5 mm
Solution PH of 10%	4-6

### 3.2. Experimental set up.

A dryer that was compatible with both fixed and fluidized bed was designed and manufactured. Figure 2 shows the schematic of the device. The adsorbent is placed inside the device and the hot air generated by a blower passes a heater and dries the adsorbent through convection heat transfer.

A blower with an adjustable flow rate of up to 200 m<sup>3</sup>/hr was installed to provide the required air. The air flow rate was measured using a flow meter in the laboratory. A heater with an adjustable temperature setting of 0 to 200° C was used to generate the required heat. The device has two temperature sensors and two humidity sensors, which provide digital and accurate readable data through displays on the panel of the device. The inlet and outlet

temperature and relative humidity were transferred online to the computer and recorded using Graph View Vista 3.0.5. The adsorbent is placed inside the bed. The height of the bed is adjustable based on the adsorbent volume.

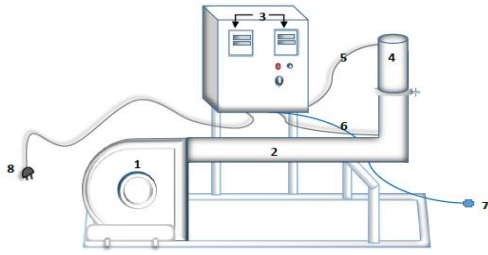


**Figure 2.** the schematic of the experimental setup: (1) Blower, (2) Heater, (3) Data Displays, (4) Stainless Steel Column with Fixed and Fluidized Bed, (5) Outlet Sensor, (6) Inlet Sensor, (7) Computer Connection Cable, (8) Power Cable.

**3.3. Methods.**

To determine the kinetic parameters of Silica gel drying, 11 experiments were conducted at different temperatures, air flow rates, and relative humidity in a fixed-bed dryer. A certain amount

of adsorbent was first weighted. This measured value is the initial weight of the adsorbent or  $W_t$ . The adsorbent was then placed in the device. The temperature and flow rate were adjusted using the switches on the device. The device was then connected to the computer and the device was turned on. Graph View Vista 3.0.5 was used to record the digitized data. Table 2 shows the operating conditions of the experiments.

**Table 2.** Operating Conditions of Experiment.

Run number	Q (m <sup>3</sup> /h)	W <sub>t</sub> (g)	T <sub>in</sub> (°C)	H <sub>R</sub> in (%)
1	15	83.147	75	9
2	42	205.1	80	8
3	27	130.941	85	8
4	38	270.213	90	8
5	43	259.023	70	7
6	30	181.53	100	6
7	40	287.397	90	8
8	35	241.19	85	8
9	20	309.334	90	6
10	31	133.846	90	7
11	33	175.571	85	7.5

**4. RESULTS AND DISCUSSION**

**4.1. Determination of the effective diffusion coefficient in bed ( $D_{eff}$ ).**

The values of the diffusion coefficient of water in the air ( $D_{A,B}$ ) were first calculated using equation (6) at different temperatures (65 to 100° C). The effective diffusion coefficient ( $D_{eff}$ ) was calculated using porosity from equation (5). Figure 3 shows the effective diffusion coefficient of water in the bed by temperature. As can be seen,  $D_{eff}$  increases with temperature. This is due to the fact that, by increasing the temperature, the internal energy of the gas molecules increases, and, as a result, the velocity of the molecules also increase.

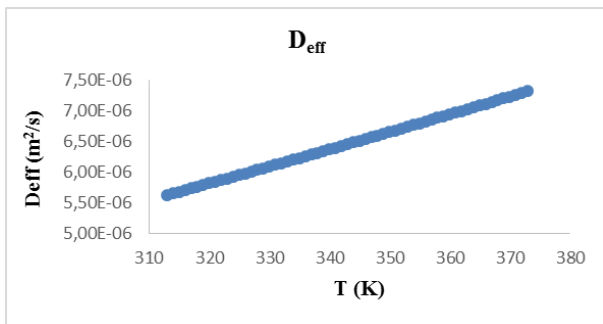


**Figure 3.** Effective Diffusion Coefficient of Water Vapor in Fixed Bed Dryer by Temperature.

**4.2. Determination of the mass transfer coefficient ( $K_C$ ).**

As mentioned before, experiments were carried out at different temperatures and air flow rates for particles with a size of 4mm, and the kinetic parameters were obtained for each temperature and air flow rate.

First, at each temperature, density, porosity, and diffusion coefficient, the dimensionless numbers were obtained. Kc was then calculated for each experiment. The statistical results of the experimental data obtained by the test design software Design Expert are presented in Table (3). The Response Surface method and the Historical Method were used for statistical analysis. Three parameters affecting the mass transfer coefficient were given to the software. Parameter A is the temperature of the air, parameter B is the air flow rate, and parameter C is the relative humidity of the inlet air. The effect of changes in the above parameters on the R2 factors of mass transfer coefficient in the fixed-bed dryer was experimentally investigated.

**Table 3.** The Experimental Results Carried Out to Determine Mass Transfer Coefficient ( $K_C$ ).

Run	Factor 1 A: Temperature C	Factor 2 B: Flow rate m3/h	Factor 3 C: Relative Humidity %	Response 2 Kc m/s
1	75.00	15.00	9.00	0.251318
2	80.00	42.00	8.00	0.394361
3	85.00	27.00	8.00	0.331048
4	90.00	38.00	8.00	0.387651
5	70.00	43.00	7.00	0.388061
6	100.00	30.00	6.00	0.35936
7	90.00	40.00	8.00	0.396195
8	85.00	35.00	8.00	0.36965
9	90.00	20.00	6.00	0.295101
10	90.00	31.00	7.00	0.345724
11	85.00	33.00	7.50	0.355485

After statistical analysis, equation (12) was obtained to estimate the mass transfer coefficient.

$$K_C = 0.34 + 0.032 A + 0.064 B + 0.019 C - 0.023 A.B \quad (12)$$

Figure 4 shows the mass transfer coefficient variations caused by the inlet air temperature. As can be seen, increased inlet air temperature increases the mass transfer coefficient.

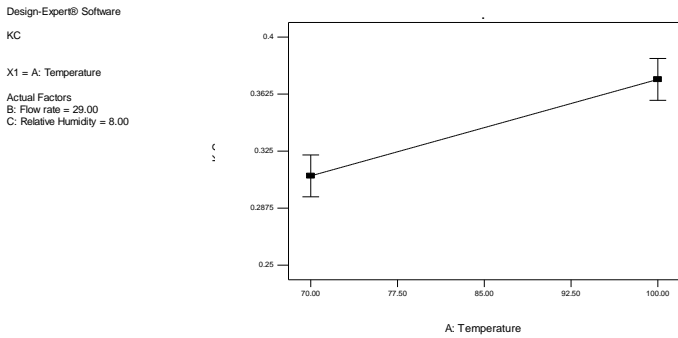


Figure 4. Mass Transfer Coefficient Variations Caused by the Inlet Air Temperature.

Figure 5 shows the mass transfer coefficient variations by the inlet air flow rate. As can be seen, increased inlet air flow rate strongly increases the mass transfer coefficient. The reason is that an increase in the air flow rate increases its velocity, which subsequently increases the Re number. The increased Re increases the dimensionless number Sh, increasing the mass transfer coefficient.

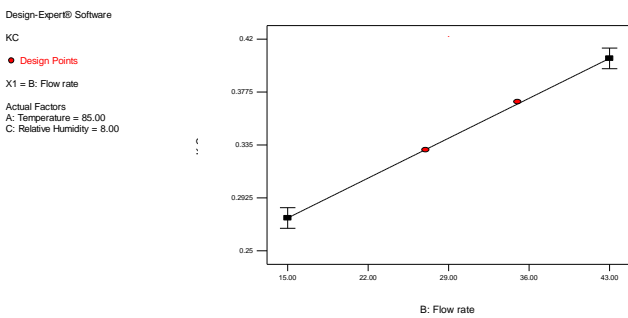


Figure 5. Mass Transfer Coefficient Variations Caused by the Inlet Air Flow Rate.

Figure 6 shows the mass transfer coefficient variations by the relative humidity of the inlet air. As can be seen, increasing the relative humidity of the inlet air increases the mass transfer coefficient.

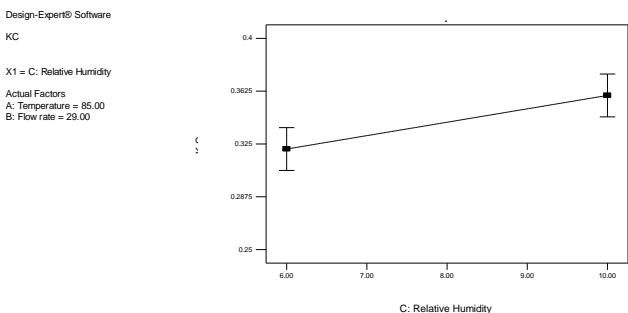


Figure 6. Mass Transfer Coefficient Variations Caused by the Inlet Air Relative Humidity.

Figures 4-6 show the individual effect of the parameters affecting the mass transfer coefficient (regardless of their

combined effect). The combined effect of the parameters is now discussed.

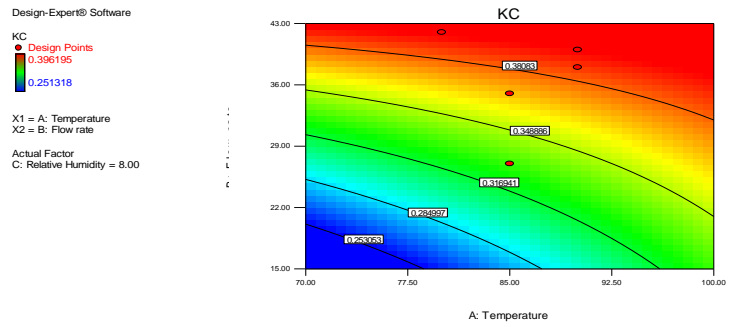


Figure 7. Effect of Simultaneous Interaction between the Parameters of Air Inlet Temperature and Inlet Air flow on Mass Transfer Coefficient.

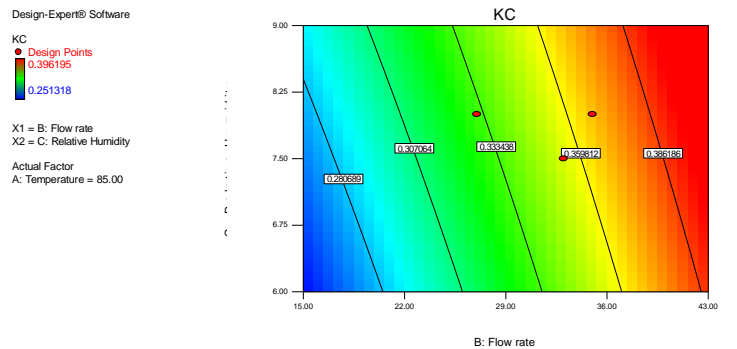


Figure 8. Effect of Simultaneous Interaction between the Parameters of Air Inlet Temperature and Relative Humidity on Mass Transfer Coefficient.

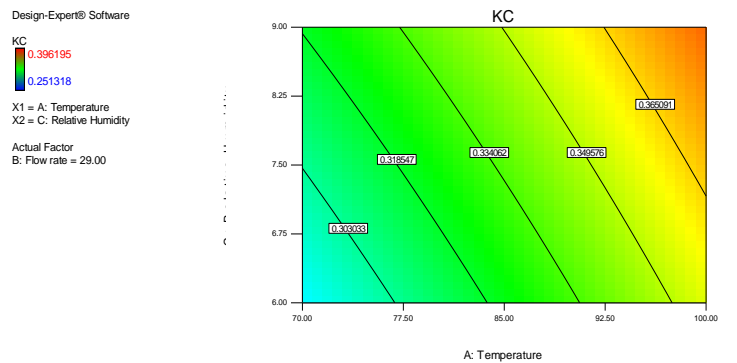


Figure 9. Effect of Simultaneous Interaction between the Parameters of Air Inlet Flow Rate and Relative Humidity on Mass Transfer Coefficient.

### 4.3. Determination of the heat transfer coefficient (h).

Equation (2) was used to calculate the theoretical heat transfer coefficient for the vertical flow of air over the particles. The Response Surface design method and the Historical Method were used for statistical analysis. Three parameters affecting mass transfer coefficient were given to the software. Parameter A, B, and C represent the temperature of the inlet air, the inlet air flow rate, and the relative humidity of the air entering the dryer, respectively. The effect of changes in these parameters on the R3 factors of mass transfer coefficient in fixed-bed dryer was experimentally investigated. These values are given in Table (4).

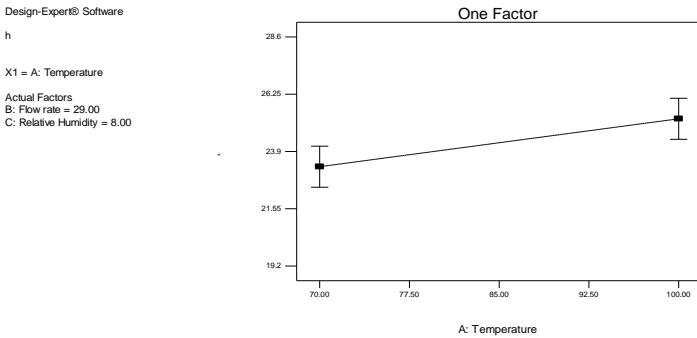
**Table 4.** Results of Experiments Carried Out to Determine the Heat Transfer Coefficient (h)

Run	Factor 1 A: Temperature C	Factor 2 B: Flow rate m3/h	Factor 3 C: Relative Humidity %	Response 3 h w/m2.K
1	75.00	15.00	9.00	19.2372
2	80.00	42.00	8.00	28.009
3	85.00	27.00	8.00	23.6614
4	90.00	38.00	8.00	26.7134
5	70.00	43.00	7.00	28.5558
6	100.00	30.00	6.00	24.2314
7	90.00	40.00	8.00	27.2252
8	85.00	35.00	8.00	26.046
9	90.00	20.00	6.00	21.0664
10	90.00	31.00	7.00	24.7749
11	85.00	33.00	7.50	25.4851

After statistical analysis, equation (13) was obtained for estimating the heat transfer coefficient:

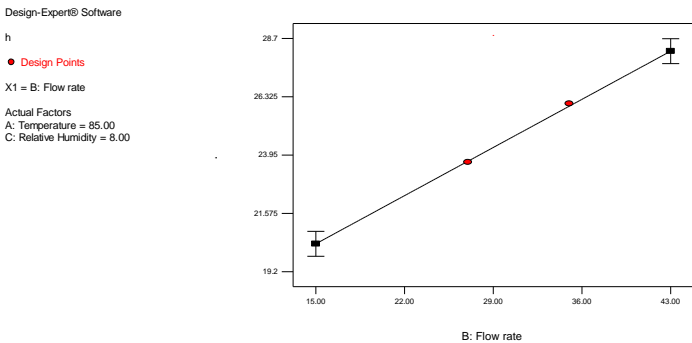
$$h = 24.26 + 0.98A + 3.92B + 0.69C - 1.26A \cdot B + 0.52A \cdot C - 0.53B \cdot C \quad (13)$$

Figure 10 shows the variations in heat transfer coefficient by the inlet air temperature. Increased inlet air temperature increased the heat transfer coefficient.



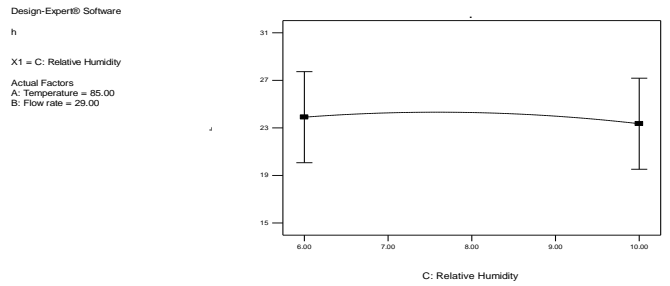
**Figure 10.** Heat Transfer Coefficient Variations Caused by the Inlet Air Temperature.

Figure 11 shows the variations in heat transfer coefficient caused by the inlet air flow rate. An increase in inlet air flow rate strongly increases the heat transfer coefficient.



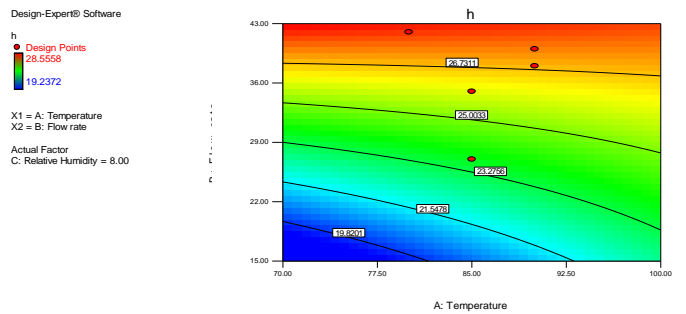
**Figure 11.** Heat Transfer Coefficient Variations Caused by the Inlet Air Flow Rate.

Figure 12 shows the variations of heat transfer coefficient caused by the relative humidity of the inlet air. As seen, increasing the inlet air relative humidity slightly increases the heat transfer coefficient.



**Figure 12.** Heat Transfer Coefficient Variations Caused by the Inlet Air Relative Humidity.

The above figures show the individual effect of the parameters affecting the mass transfer coefficient (regardless of the interaction between them). The combined effect of the parameters is now discussed.



**Figure 13.** Simultaneous Effect of Inlet Air Temperature and Flow Rate on the Heat Transfer Coefficient.

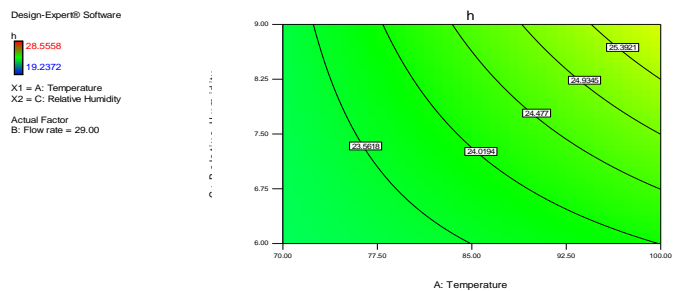


**Figure 14.** Simultaneous Effect of Inlet Air Temperature and Relative Humidity on the Heat Transfer Coefficient.

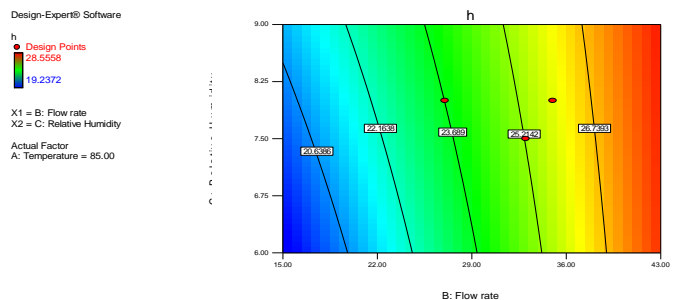


**Figure 15.** Simultaneous Effect of Inlet Air Flow Rate and Relative Humidity on the Heat Transfer Coefficient

## 5. CONCLUSION

In this study, variations in heat and mass transfer caused by temperature, humidity, and air flow rate were studied simultaneously in the silica gel drying process in a fixed-bed dryer. An empirical-mathematical relation was obtained for predicting the mass transfer coefficient as well as an empirical-mathematical relation for predicting the heat transfer coefficient in fixed-bed drying. Experimental results showed that higher silica gel moisture content leads to a greater drying rate. As the

temperature increases, the diffusion rate of water vapor in the air and the effective diffusion coefficient are increased. Raising the temperature from 80°C to 100°C, at flow rates of 40 to 42 m<sup>3</sup>/h increases the mass transfer coefficient. Experimental data showed that raising the temperature from 70°C to 90°C, at flow rates of 40 to 43 m<sup>3</sup>/h increases the heat transfer coefficient. An increase in relative humidity of the air results in a decrease in the mass transfer coefficient.

## 6. REFERENCES

- [1] Stramilo S., Codor T., Drying, principles, application and design, Tehran, TarbiatModares University, Scientific Research Center, **1986**.
- [2] Dobre T., Părvulesc, O. C., Guzun A. S., Stroescu M., Jipa I., Al Janabi A. A., "Heat and Mass Transfer in Fixed Bed Drying of Non-Deformable Porous Particles, *International Journal of Heat and Mass Transfer*, 103, 478-485, **2016**.
- [3] Perkin R.M., Drying of Porous Materials with Electromagnetic Energy Generated at Radio and Microwave Frequencies ECRC Report, The Electricity Council Research Centre, Capenhurst, *Chester CHIGES, Report No. ECRC/M1646*, **1983**.
- [4] Souza G.F.M.V., Miranda R.F., Lobato F.S., Barrozo M.A.S., Simultaneous heat and mass transfer in a fixed bed dryer, *Applied Thermal Engineering*, 90, 38-44, **2015**.
- [5] Roman F., Schafer V. S., Hensel O., Improvement of air distribution in a fixed-bed dryer using computational fluid dynamics, *Biosystems Engineering*, 112, 359-369, **2012**.
- [6] Hashemi M., Ghavidel M., GilaniGhanadzade, H., Parsley drying kinetics using fixed bed and sunlight dryers and modeling using artificial neural network, *15th National Congress of Chemical Engineering*, Tehran, Tehran University, **2014**.
- [7] Rahmanian H., Koushkaki A., Moghadami N., Zare D., Karimi, G., Experimental and Theoretical Investigation of Hot Air- Infrared Thin Layer Drying of Corn in a Fixed and Vibratory Bed Dryer, *Engineering in Agriculture, Environment and Food*, In Press, Corrected Proof, **2017**.
- [8] Pusat S., TahirAkkoyunlu M., Hussein Erdem H., Dağdaş A., Drying kinetics of Coarse Lignite Particles in a Fixed Bed, Yildiz Technical University, Department of Mechanical Engineering, Istanbul, Turkey, **2015**.
- [9] Tohidi M., Sadeghi M. Toriki-Harchegani M., Energy and Quality Aspects for Fixed Deep Bed Drying of Paddy, *Renewable and Sustainable Energy Reviews*, 70, 519-528, **2017**
- [10] Craft B. C., Hawkins M. F., *Petroleum Reservoir Engineering*, Prentice Hall Inc., **1973**.
- [11] Riazi M. R., Whitson C. H., da Silva F., Modelling of diffusional mass transfer in naturally fractured reservoirs, *Journal of Petroleum Science and Engineering*, 10, 239-253, **1994**.
- [12] Treybal, R. E., *Mass transfer operations*, New York, **1980**
- [13] Stynes S. K. Myers J. E., Transport from extended surfaces, *AIChE Journal*, 10, 4, 437-444, **1964**.
- [14] Tan A. Y., Prushen B. D., Guin J. A., *AIChE Journal*, 21, 396, **1975**.
- [15] Chilton T. H., Colburn A. P., Mass transfer (absorption) coefficients prediction from data on heat transfer and fluid friction, *Industrial & engineering chemistry*, 26, 11, 1183-1187, **1934**
- [16] De Leersnyder F., Vanhoorne V., Bekaert H., Vercruyse J., De Beer T., Breakage and drying behaviour of granules in a continuous fluid bed dryer: Influence of process parameters and wet granule transfer, *European Journal of Pharmaceutical Sciences*, 115, 223-232, **2018**.
- [17] Moran S., *Process Plant Layout*, 2nd ed., Butterworth-Heinemann, 419-440, **2017**.
- [18] Bird R. B., Stewart W. E., Lightfoot, E. N., *Transport Phenomena*, Wiley, New York, **1960**.
- [19] Mohammed R. H., Mesalhy O., Elsayed M. L., Hou S., Chow L.C., Physical properties and adsorption kinetics of silica-gel/water for adsorption chillers, *Applied Thermal Engineering*, 137, 368-376, **2018**.